Liquid Crystals
Publication details, including instructions for authors and subscription information:
http://www.informaworld.com/smpp/title~content=t713926090

Application of a generalised thermodynamic model to study of the ferroelectric properties of DOBAMBC and DOBA-1-MPC

Abhilasha Singh[a]; Shri Singh[a]
[a] Department of Physics, Banaras Hindu University, Varanasi-221 005, India

To cite this Article Singh, Abhilasha and Singh, Shri(2008) 'Application of a generalised thermodynamic model to study of the ferroelectric properties of DOBAMBC and DOBA-1-MPC', Liquid Crystals, 35: 6, 727 — 736
To link to this Article: DOI: 10.1080/02678290802120315
URL: http://dx.doi.org/10.1080/02678290802120315

Liquid Crystals,
Vol. 35, No. 6, June 2008, 727–736

Taylor & Francis
Taylor & Francis Group

Application of a generalised thermodynamic model to study of the ferroelectric properties of DOBAMBC and DOBA-1-MPC

Abhilasha Singh and Shri Singh*

Department of Physics, Banaras Hindu University, Varanasi-221 005, India

(Received 11 January 2008; accepted 10 April 2008)

The temperature variations of tilt angle, spontaneous polarisation, helical pitch, Goldstone mode rotational viscosity and twist elastic constant of the ferroelectric smectic C (SmC*) phase near the smectic A (SmA)–SmC* transition of the ferroic mesogens DOBAMBC and DOBA-1-MPC were calculated using a thermodynamic model based on an extended Landau expansion of the free-energy density. The model free-energy density of the system is written in terms of order parameters (tilt vector ξ, polarisation **P** and wavevector q of helical pitch) involving eleven mean-field coefficients including bilinear, biquadratic and flexoelectric couplings between ξ and **P** and coefficients due to coupling between ξ and q. The values of these coefficients were determined by fitting the results of calculation with the experimental data for the pitch, tilt angle and spontaneous polarisation. A detailed analysis of the relative contribution of each individual term appearing in the free-energy density expansion is presented. Taking these values of parameters, in addition to tilt angle, spontaneous polarisation and pitch, we calculate the Goldstone mode rotational viscosity and twist elastic constant as a function of temperature. The theoretical results agree well with the experimental data for both mesogens.

Keywords: thermodynamic model; ferroelectric liquid crystal

1. Introduction

Mesogenic materials exhibiting the helicoidal chiral smectic C (SmC*) phase have been the subject of considerable interest (*1–6*) in fields of condensed matter physics and statistical mechanics and much effort has been spent on investigating their behaviour from both fundamental as well as potential application (*7, 8*) viewpoints. Meyer *et al.* (*9*) were the first to establish the existence and investigate the behaviour of the ferroelectric SmC* phase in a mesogen, 4-*n*-decyloxybenzilidene-4′-amino-2-methylbutyl cinnamate (DOBAMBC). Since then a range of experimental data for the tilt angle, polarisation, helical pitch and other physical properties have become available for DOBAMBC (*10–20*), the related compound 4-*n*-decyloxybenzilidene-4′-amino-1-methylpropyl cinnamate (DOBA-1-MPC) (*18–21*) and other mesogenic ferroic materials (*22–30*). However, little is understood about the basic thermodynamic functions of the SmC* phase and the properties of the smectic A (SmA)–SmC* phase transition. Most theoretical attempts have been based on the phenomenological Landau type expansion (*31–36*) of the free-energy density near the SmA–SmC* transition.

The ferroelectric liquid crystals DOBAMBC and DOBA-1-MPC exhibit the following cooling phase sequences:

I 117 SmA 94.5 SmC $*$ (63 SmI)75 Cr(DOBAMBC);

I 116 SmA 86.0 SmC $*$ (61 SmI)82 Cr(DOBA$-$1$-$MPC),

where the numbers are transition temperatures in °C and I and Cr represent, respectively, the isotropic liquid and crystalline phases. Measurements of high-resolution heat capacity, tilt angle (θ_0) and spontaneous polarisation (P_0) were carried out near the SmA–SmC* phase transition by Dumrongrattana *et al.* (*12*). They measured θ_0 and P_0 almost simultaneously using an electro-optical technique and the measurement of displacement current through the field-reversal method, respectively, and found that the ratio P_0/θ_0 stays fairly constant for $T_c - T > 2$ K and drops precipitously near the transition temperature T_c. An alternative method, based on the dielectric measurements on thick samples, was used by Levstik *et al.* (*21*) to study the temperature dependence of the tilt angle, spontaneous polarisation, helical pitch, Goldstone mode rotational viscosity and twist elastic constant of DOBAMBC and DOBA-1-MPC. We have used the experimental results of these authors (*21*) in this work.

The temperature variations of the tilt angle, polarisation and their ratio and pitch in DOBAMBC were investigated by Huang and Dumrongrattana (*32*) using the generalised mean-field model, which is similar to that proposed by Zeks (*33*). They determined the model parameters by fitting to the experimental data (*12*) and found that the values of the tilt angle, spontaneous polarisation and their ratio are described well by the model, but

*Corresponding author. Email: srisingh23@gmail.com

ISSN 0267-8292 print/ISSN 1366-5855 online

DOI: 10.1080/02678290802120315
http://www.informaworld.com

the fitting to the helical pitch was less satisfactory. In the case of DOBA-1-MPC there is so far, as known to us, no systematic theoretical study to describe the characteristic features of SmA–SmC* transition properties. The purpose of the present work is to provide, using the generalised Landau mean-field model, a comprehensive description of the temperature variations of the tilt angle, spontaneous polarisation, helical pitch, heat capacity, Goldstone mode rotational viscosity and twist elastic constant in the SmC* phase near the SmA–SmC* transition in DOBAMBC and DOBA-1- MPC. It is pertinent to mention here that our theoretical results of the heat capacity, tilt angle and spontaneous polarisation for the DOBAMBC are in good agreement with experiment (*21*) and similar to the results of Huang and Dumrongrattana (*32*). These authors (*32*) obtained a qualitative agreement for the temperature variation of the pitch of DOBAMBC with experimental data (*10, 11*), but we obtain a close agreement with other experimental data (*21*). Our results for Goldstone mode rotational viscosity and twist elastic constant of DOBAMBC and all the results for DOBA-1-MPC are new and agree very well with experiment (*21*). The paper is organised as follows. In section 2, we describe, in brief, the thermodynamic model used here and obtain the equations for the equilibrium values of pitch, tilt angle and spontaneous polarisation. The numerical calculations and results are given in section 3. The paper ends with a summary and conclusion together with the possible outlook in section 4.

2. Theoretical framework and working equations

The present work is based on an extended thermodynamic model of the SmC* phase near the SmA–SmC* transition in which the free-energy density is written as an expansion in terms of order parameters. A full review on this model is given elsewhere (*34*). However, for the sake of completeness, we present here a brief summary.

A brief description of the generalised mean-field model

The theoretical description of the SmA–SmC* phase transition is based on the introduction of two-component order parameters related with the tilt vector, $\boldsymbol{\xi}=(\xi_1, \xi_2)$ and in-plane polarisation, $\mathbf{P}=(P_x, P_y)$ (*34–36*). In the SmC* phase the tilt of the director vector $\hat{\mathbf{n}}$ from the normal to the smectic layers processes helically as one goes from one smectic layer to the another. The projection of $\hat{\mathbf{n}}$ into the plane of a smectic layer is described by the primary order parameter (tilt vector) $\boldsymbol{\xi}_{-}=\xi_1\hat{\mathbf{x}}+\xi_2\hat{\mathbf{y}}$. Because of the chirality of the molecules the tilt breaks the axial symmetry around the molecular axis and induces a transverse in-plane polarisation (secondary order parameter) $\mathbf{P}=P_x\hat{\mathbf{x}}+P_y\hat{\mathbf{y}}$ perpendicular to $\hat{\mathbf{n}}$. Figure 1 defines the order parameters $\boldsymbol{\xi}$ and $\mathbf{P}$. The smectic planes are assumed to be parallel to the xy plane and the modulation of the system is along the z-axis.

The free-energy density of a SmC* phase in the vicinity of the SmA–SmC* transition is written (*34–36*) as an expansion in terms of order parameters $\boldsymbol{\xi}$ and $\mathbf{P}$:

$$\begin{aligned} g_0(z) = {} & \frac{1}{2}a\left(\xi_1^2+\xi_2^2\right)+\frac{1}{4}b\left(\xi_1^2+\xi_2^2\right)^2+\frac{1}{6}c\left(\xi_1^2+\xi_2^2\right)^3 \\ & -\Lambda\left[\xi_1\frac{\mathrm{d}\xi_2}{\mathrm{d}z}-\xi_2\frac{\mathrm{d}\xi_1}{\mathrm{d}z}\right]+\frac{1}{2}K_3\left[\left(\frac{\mathrm{d}\xi_1}{\mathrm{d}z}\right)^2+\left(\frac{\mathrm{d}\xi_2}{\mathrm{d}z}\right)^2\right] \\ & +\frac{1}{2\chi}\left(P_x^2+P_y^2\right)+Z\left(P_x\xi_2-P_y\xi_1\right) \\ & -f\left[P_x\,\mathrm{d}\xi_1/\mathrm{d}z+P_y\,\mathrm{d}\xi_2/\mathrm{d}z\right] \\ & -\frac{1}{2}e\left(P_x\xi_2-P_y\xi_1\right)^2+\frac{1}{4}\eta\left(P_x^2+P_y^2\right)^2 \\ & -d\left(\xi_1^2+\xi_2^2\right)\left(\xi_1\,\mathrm{d}\xi_2/\mathrm{d}z-\xi_2\,\mathrm{d}\xi_1/\mathrm{d}z\right). \end{aligned} \tag{1}$$

Only the coefficient a of the term quadratic in tilt is assumed to be temperature dependent and goes to zero at the 'unrenormalised' transition temperature T_0 for a ferroelectric liquid crystal (FLC), i.e. $a=a_0(T-T_0)$. All the other coefficients are taken to be temperature independent. χ is the generalised susceptibility, K_3 is the elastic modulus, Λ is the coefficient of the Lifshitz invariant term responsible for the helical structure, f and Z are the coefficients of the flexo- and piezoelectric bilinear coupling between the tilt and the polarisation, respectively. e is the coefficient of the biquadratic coupling term inducing transverse quadrupole ordering and the η term has been included for the stability of the system. The d

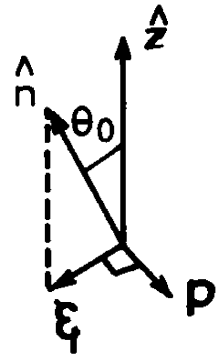

Figure 1. Introduction of the order parameters ξ and $\mathbf{P}$.

term describes the monotonic increase of the pitch with temperature at low temperature. The first two terms (with coefficients a and b) in Equation (1) are the usual quadratic and fourth-order terms in the tilt, which appear in the free-energy density expansion of a system close to a second-order phase transition. For physical reasons, the parameters a, b, c, K_3, χ and η can be assumed to be positive, whereas the sign of Λ, f, Z, e and d can be permitted to assume both positive and negative values.

Equation (1) was first introduced by Zeks (*33*), except for the six-order term in the tilt, which was independently introduced by Huang and Viner (*37*) and by Carlsson and Dahl (*38*). We can obtain the "classical" Landau model (*31*) for the free-energy density from Equation (1) by putting the terms with parameters c, e, η and d equal to zero. The most important characteristic feature of the generalised mean-field model, in contrast to the classical one, is the presence of the biquadratic coupling (the e term) between the tilt and polarisation. This term, first introduced by Zeks (*33*), describes the fact that the tilt induces a transverse quadrupole moment in chiral as well as achiral SmC phases, and its inclusion in Equation (1) is essential in order to describe correctly the anomalous thermodynamic properties of FLCs (temperature dependence of helical pitch, dielectric susceptibility, critical electric field for the unwinding of pitch, etc.).

As the tilt is small near the SmA–SmC* transition, we can assume $|\xi|=\sin\theta_0\approx\theta_0$ (tilt angle). The polarisation is always mutually perpendicular to both $\boldsymbol{\xi}$ and $\hat{\mathbf{z}}$. For a given $\boldsymbol{\xi}$ and $\hat{\mathbf{z}}$, $\mathbf{P}$ can assume two possible directions. When $\boldsymbol{\xi}$, $\mathbf{P}$ and $\hat{\mathbf{z}}$ form a right-handed coordinate system, the compound is said to be a (+) substance and if they form a left-handed system we have a (−) substance. Defining the wavevector of pitch $q=2\pi/p$ we assume for the order parameters

$$\begin{aligned} \xi_1 &= \theta_0\cos(qz), \qquad \xi_2 = \theta_0\sin(qz), \\ P_x &= -P_0\sin(qz), \quad P_y = P_0\cos(qz), \end{aligned} \tag{2}$$

where θ_0 and P_0 are the magnitudes of the tilt angle and the spontaneous polarisation, respectively.

Substituting Equation (2) into Equation (1), we obtain the expression for the Gibbs-free energy density of the SmC* phase in the vicinity of SmA–SmC* transition (*33, 34*)

$$\begin{aligned} g_0(z) = {} & \frac{1}{2}a\theta_0^2 + \frac{1}{4}b\theta_0^4 + \frac{1}{6}c\theta_0^6 - \Lambda q\theta_0^2 + \frac{1}{2}K_3q^2\theta_0^2 + \frac{1}{2\chi}P_0^2 \\ & - ZP_0\theta_0 - fqP_0\theta_0 - \frac{1}{2}eP_0^2\theta_0^2 + \frac{1}{4}\eta P_0^4 - dq\theta_0^4. \end{aligned} \tag{3}$$

The equilibrium values of θ_0, P_0 and q are determined from the condition that g_0 should be a minimum with respect to all these variables.

Equations governing pitch, tilt and polarisation

We derive the equations governing the pitch, tilt angle and polarisation of an unperturbed SmC* phase by minimising Equation (3) with respect to q, θ_0 and P_0, respectively. For q, we obtain

$$q = \frac{1}{K_3}\left(\Lambda + \mathrm{d}\theta_0^2 + fP_0/\theta_0\right). \tag{4}$$

Thus the pitch is a function of the tilt and the polarisation. We obtain the tilt equation by minimising Equation (3) with respect to θ_0,

$$\begin{aligned} c\theta_0^5 + (b - 4\,\mathrm{d}q)\theta_0^3 + \left(a - 2\Lambda q + K_3q^2 - eP_0^2\right)\theta_0 - \\ (Z + fq)P_0 = 0. \end{aligned} \tag{5}$$

Minimisation of Equation (3) with respect to P_0 gives the polarisation equation

$$\eta P_0^3 + \left(1/\chi - e\theta_0^2\right)P_0 - (Z + fq)\theta_0 = 0. \tag{6}$$

Substituting for q [Equation (4)] in Equation (3), $g_0(z)$ can be written in terms of only θ_0 and P_0

$$\begin{aligned} g_0(z) = {} & \frac{1}{2}\left(a_2(T - T_0) - \Lambda^2/K_3\right)\theta_0^2 + \frac{1}{4}a_4\theta_0^4 + \frac{1}{6}a_6\theta_0^6 \\ & + \frac{1}{2}\alpha P_0^2 + \frac{1}{4}\eta P_0^4 - \beta P_0\theta_0 - \gamma_0 P_0\theta_0^3 - \frac{1}{2}eP_0^2\theta_0^2, \end{aligned} \tag{7}$$

where the new Landau coefficients are defined as

$$\begin{aligned} a_2 &= a_0 \\ a_4 &= b - 4\Lambda d/K_3 \\ a_6 &= c - 3d^2/K_3 \\ \alpha &= 1/\chi - f^2/K_3 \\ \beta &= Z + \Lambda f/K_3 \end{aligned}$$

and

$$\gamma_0 = df/K_3. \tag{8}$$

Minimising Equation (7) with respect to θ_0 and P_0, the tilt angle and polarisation equations are obtained as

$$\begin{aligned} & a_6\theta_0^5 + a_4\theta_0^3 - 3\gamma_0 P_0\theta_0^2 + \left[a_2(T - T_0) - \Lambda^2/K_3 - eP_0^2\right]\theta_0 \\ & - \beta P_0 = 0 \end{aligned} \tag{9}$$

and

$$\eta P_0^3 + (\alpha - e\theta_0^2) P_0 - \beta\theta_0 - \gamma_0\theta_0^3 = 0. \quad (10)$$

An expression for the SmA–SmC* transition temperature T_c can be obtained from the fact that at the transition both P_0 and θ_0 tend to vanish such that the ratio P_0/θ_0 remains finite. In this limit, Equation (9) reads

$$a_2(T_c - T_0) - \Lambda^2/K_3 - \beta\left(\frac{P_0}{\theta_0}\right)\Big|_{T\to T_c} = 0. \quad (11)$$

Taking the limit $T \to T_c$ in Equation (10), we obtain

$$\alpha\left(\frac{P_0}{\theta_0}\right)\Big|_{T\to T_c} - \beta = 0. \quad (12)$$

Thus, the ratio P_0/θ_0 at the phase transition is given by

$$lim_{T\to T_c}\left(\frac{P_0}{\theta_0}\right) = \beta/\alpha. \quad (13)$$

Substitution of Equation (13) into Equation (11) gives

$$T_c = T_0 + \frac{1}{a_2}\left[\frac{\Lambda^2}{K_3} + \frac{\beta^2}{\alpha}\right]. \quad (14)$$

This shows that the SmA–SmC* transition temperature is slightly shifted for the SmC* phase in comparison with its racemic mixture.

Influence of electric field: Goldstone mode rotational viscosity and twist elastic constant of the SmC phase*

In an undistorted SmC* phase, the direction of polarisation **P** spirals around the smectic layer normal $\hat{\mathbf{z}}$ because of the helical variation of the tilt direction and the net polarisation is zero. When an electric field of magnitude E is applied parallel to the smectic layers, it deforms the helix in such a way that an average macroscopic polarisation $<\mathbf{P}_i>$ is induced. The dielectric susceptibility χ is then defined as

$$\chi(\omega) = \lim_{E\to 0}\frac{\langle \mathbf{P}_i \rangle}{E}. \quad (15)$$

The applied field deforms the helix in two ways; changing the magnitude as well as direction of the tilt. Both the amplitude and the phase of the order parameters $\boldsymbol{\xi}$ and **P** will be influenced by the field so that the sinusoidal ansatz of Equation (2) will no longer be valid. Denoting the amplitude changes by $\delta\theta_1$ and δP_1 and phase changes by $\delta\theta_2$ and δP_2, respectively, one can write the following ansatz for the order parameters in the presence of an electric field (*34, 35*)

$$\begin{aligned}
\xi_1 &= \theta_0\cos(qz) + \delta\theta_1\cos(qz) - \delta\theta_2\sin(qz),\\
\xi_2 &= \theta_0\sin(qz) + \delta\theta_1\sin(qz) + \delta\theta_2\cos(qz),\\
P_x &= -P_0\sin(qz) - \delta P_1\sin(qz) - \delta P_2\cos(qz),\\
P_y &= P_0\cos(qz) + \delta P_1\cos(qz) - \delta P_2\sin(qz).
\end{aligned} \quad (16)$$

Thus, the dielectric response has been divided into two modes, one which is due to amplitude changes (soft mode) and another which is due to phase changes (Goldstone mode) of the order parameters. This division, however, is not clear-cut because of a small amplitude-phase coupling. The amplitude-phase coupling is so small that to a good approximation the two modes can be defined as

$$\chi_1 = \lim_{E\to 0}\frac{\langle \boldsymbol{P}_{i1} \rangle}{E}, \qquad \text{(soft mode)} \quad (17)$$

$$\chi_2 = \lim_{E\to 0}\frac{\langle \boldsymbol{P}_{i2} \rangle}{E}, \qquad \text{(Goldstone mode)} \quad (18)$$

where $<\mathbf{P_{i1}}>$ and $<\mathbf{P_{i2}}>$ are the averages of the amplitude part and the phase part of the induced polarisation, respectively.

We assume that the electric field is applied parallel to the smectic layers and that the electric field has a time dependence $\mathbf{E} = E_0\exp(j\omega t)\hat{\mathbf{x}}$. Substituting ansatz (16) into Equation (1), the free-energy density can be written as

$$g(z) = g_0(z) + g_2(z) + g_E(z), \quad (19)$$

where $g_0(z)$ is given by the Equation (1), $g_2(z)$ is the extra contribution due to the changes of the order parameters and $g_E(z)$ is the contribution due to the electric field. Retaining terms quadratic in $\delta\theta$ and δP, we obtain

$$\begin{aligned}
g_2(z) = {} & \delta\theta_1^2\left(\frac{1}{2}a + \frac{3}{2}b\theta_0^2 + \frac{5}{2}c\theta_0^4 - \Lambda q + \frac{1}{2}K_3q^2\right.\\
& \left. - \frac{1}{2}eP_0^2 - 6\,\mathrm{d}q\theta_0^2\right) + \delta\theta_2^2\left(\frac{1}{2}a + \frac{1}{2}b\theta_0^2 + \frac{1}{2}c\theta_0^4 - \Lambda q\right.\\
& \left. + \frac{1}{2}K_3q^2 - 2\,\mathrm{d}q\theta_0^2\right) + \delta P_1^2\left(\frac{1}{2\chi} - \frac{1}{2}e\theta_0^2 + \frac{3}{2}\eta P_0^2\right)\\
& + \delta P_2^2\left(\frac{1}{2\chi} + \frac{1}{2}\eta P_0^2\right) - \delta\theta_1\delta P_1(fq + Z + 2eP_0\theta_0)\\
& - \delta\theta_2\delta P_2(fq + Z + eP_0\theta_0) + \delta\theta_1\delta\theta'_2\left(-\Lambda + K_3q - 3\,\mathrm{d}\theta_0^2\right)\\
& + \delta\theta'_1\delta\theta_2\left(\Lambda - K_3q + \mathrm{d}\theta_0^2\right) + \frac{1}{2}K_3\left(\delta\theta'^2_1 + \delta\theta'^2_2\right)\\
& + f(\delta P_2\delta\theta'_1 - \delta P_1\delta\theta'_2)
\end{aligned} \quad (20)$$

and

$$g_E(z) = -\mathbf{E}\cdot\mathbf{P} = E_0(P_0\sin(qz) + \delta P_1\sin(qz) + \delta P_2\cos(qz))\exp(j\omega t). \quad (21)$$

Here, a prime denotes a derivative with respect to the z-coordinate. In the limit of small electric field, the space variation of $\delta\theta$ and δP can be written as (*35*)

$$\begin{aligned}\delta\theta_1 &= \delta\theta_{10}\sin(qz)\exp(j\omega t),\\ \delta\theta_2 &= \delta\theta_{20}\cos(qz)\exp(j\omega t),\end{aligned} \quad (22)$$

$$\begin{aligned}\delta P_1 &= \delta P_{10}\sin(qz)\exp(j\omega t),\\ \delta P_2 &= \delta P_{20}\cos(qz)\exp(j\omega t).\end{aligned} \quad (23)$$

Applying the Euler–Lagrange equations to the $g_2(z)$ and $g_E(z)$ terms, the following equations governing the changes of order parameters in the static limit (ω=0) are obtained

$$b_1\delta\theta_{10} + b_2\delta\theta_{20} + b_3\delta P_{10} + b_4\delta P_{20} = 0, \quad (24)$$

$$b_2\delta\theta_{10} + b_5\delta\theta_{20} + b_4\delta P_{10} + b_6\delta P_{20} = 0, \quad (25)$$

$$b_3\delta\theta_{10} + b_4\delta\theta_{20} - b_7\delta P_{10} = E_0 \quad (26)$$

$$b_4\delta\theta_{10} + b_6\delta\theta_{20} - b_8\delta P_{20} = E_0 \quad (27)$$

where

$$\begin{aligned}b_1 &= -a - 3b\theta_0^2 - 5c\theta_0^4 + 2\Lambda q - 2K_3q^2 + eP_0^2 + 12\,\mathrm{d}q\theta_0^2,\\ b_2 &= -2\Lambda q + 2q^2K_3 - 4\,\mathrm{d}q\theta_0^2,\\ b_3 &= fq + Z + 2eP_0\theta_0,\\ b_4 &= -fq,\\ b_5 &= -a - b\theta_0^2 - c\theta_0^4 + 2\Lambda q - 2K_3q^2 + 4\,\mathrm{d}q\theta_0^2,\\ b_6 &= fq + Z + eP_0\theta_0,\\ b_7 &= \frac{1}{\chi} - e\theta_0^2 + 3\eta P_0^2,\\ b_8 &= \frac{1}{\chi} + \eta P_0^2.\end{aligned}$$

In the case of the dielectric response at finite ω, the dynamic equations have to be formulated as a set of balanced torque equations,

$$\Gamma_{elastic} + \Gamma_{viscous} = 0. \quad (28)$$

Equations (26) and (27) represent the elastic torque $\Gamma_{elastic}$. The time derivatives of the order parameters give the viscous torque

$$\Gamma_{viscous} = -\gamma\delta\dot{\theta}_1 = -j\omega\gamma\delta\theta_{10}\sin(qz)\exp(j\omega t).$$

Now, adding the terms of the type $-j\omega\gamma\delta\theta_{10}$ to Equations (24)–(27) gives the dynamic equations of the system

$$(b_1 - j\omega\gamma_S)\delta\theta_{10} + b_2\delta\theta_{20} + b_3\delta P_{10} + b_4\delta P_{20} = 0, \quad (29)$$

$$b_2\delta\theta_{10} + (b_5 - j\omega\gamma_G)\delta\theta_{20} + b_4\delta P_{10} + b_6\delta P_{20} = 0, \quad (30)$$

$$b_3\delta\theta_{10} + b_4\delta\theta_{20} - (b_7 + j\omega\gamma_{PS})\delta P_{10} = E_0, \quad (31)$$

$$b_4\delta\theta_{10} + b_6\delta\theta_{20} - (b_8 + j\omega\gamma_{PG})\delta P_{20} = E_0. \quad (32)$$

These equations contain four different viscosities: γ_S, γ_G, γ_{PS} and γ_{PG}. γ_S and γ_G correspond to the director orientations, whereas remaining two, γ_{PS} and γ_{PG}, connected with the polarisation modes are due to the rotation of the molecules around their long axis. Near T_c it is expected (*36*) that γ_S=γ_G. The director modes are of much lower frequency than the polarisation modes. So the eigenfrequencies of the polarisation modes can be assumed to be infinite, i.e. γ_{PS} and γ_{PG} can be taken to be zero in Equations (31) and (32). Substituting for δP_{10} and δP_{20} into Equations (29) and (30) and diagonalising the resulting equations, we obtain (*39*) the equation determining the eigenfrequencies of the director modes of the system

$$(X + j\omega\gamma_S)(Y + j\omega\gamma_G) = 0, \quad (33)$$

where

$$X = -b_1 - \frac{b_4^2}{b_8} - \frac{b_3^2}{b_7}$$

and

$$Y = q^2\left[K_3 - \left(\frac{f^2}{\frac{1}{\chi} - e\theta_0^2 + 3\eta P_0^2}\right)\right] = q^2\widetilde{K}_3,$$

where $\widetilde{K}_3 = K_3 - f^2/\left(1/\chi - e\theta_0^2 + 3\eta P_0^2\right)$ is the renormalised elastic constant. The eigenfrequencies of the soft mode and the Goldstone mode can be obtained,

respectively, as

$$X + j\omega\gamma_S = X(1 + j\omega\tau_s)$$

and

$$Y + j\omega\gamma_G = Y(1 + j\omega\tau_G).$$

The corresponding eigenfrequencies are given as

$$f_S = 1/2\pi\tau_S = \frac{X}{2\pi\gamma_S} \tag{34}$$

and

$$f_G = 1/2\pi\tau_G = \frac{Y}{2\pi\gamma_G} = \frac{q^2\widetilde{K}_3}{2\pi\gamma_G}. \tag{35}$$

Assuming that the dielectric susceptibility corresponding to Goldstone mode can be written as

$$\chi_2 = \epsilon_0\Delta\epsilon_G/(1 + j\omega\tau_G),$$

where ϵ_0 is the permittivity of the free space and $\Delta\epsilon_G$ is the dielectric constant. We can write the Goldstone mode dielectric strength as

$$\epsilon_0\Delta\epsilon_G = \frac{1}{2\widetilde{K}_3}\left(\frac{P_0}{q\theta_0}\right)^2. \tag{36}$$

Multiplying the relaxation frequency with the dielectric strength of the Goldstone mode we obtain expression for the Goldstone mode rotational viscosity

$$\gamma_G = \left(\frac{1}{4\pi\epsilon_0}\right)\left(\frac{P_0^2}{\theta_0^2\Delta\epsilon_G f_G}\right). \tag{37}$$

Using the known values of P_0, θ_0, p, f_G and $\Delta\epsilon_G$, the γ_G and K_3 can be determined from Equations (37) and (36), respectively.

3. Numerical calculations and results

Out of the two rotational viscosities (γ_S and γ_G) the γ_G is the one that controls the switching time in an electro-optical device. The γ_G is usually measured using thick samples by optical switching–time measurements (*40, 41*) or by the polarisation reversal current technique (*41, 42*). As mentioned in section 1, Levstik *et al.* (*21*) measured the temperature dependence of the spontaneous polarisation, tilt angle and pitch and the frequency and temperature variations of the complex dielectric constant of DOBAMBC and DOBA-1-MPC. The tilt angle was measured by the conventional crossed polariser method at a constant field, whereas the spontaneous polarisation was determined simultaneously with a Sawyer–Tower bridge at 70 Hz. Both of these methods are dynamic, but allow the determination of static quantities P_0 and θ_0. The P_0 was determined by extrapolating the saturated part of the hysteresis loop to zero-field. The helical pitch was determined by the use of a polarising microscope. From the data of the complex dielectric constant the temperature variation of the dielectric strength $\Delta\epsilon_G$ of the Goldstone mode and the corresponding relaxation frequency f_G were determined. Using the data of P_0, θ_0, p, $\Delta\epsilon_G$ and f_G, they (*21*) obtained the γ_G and K_3. The K_3 was found to be approximately temperature independent except for $T_c - T \leqslant 1.5$ K. The dielectric method has the advantage that only small oscillations of the director are excited.

For the numerical calculations, we require values of 11 mean-field coefficients. We have determined these coefficients for DOBAMBC and DOBA-1-MPC by carrying out the least square fittings to the experimental data (*21*) of p, P_0, θ_0 and P_0/θ_0. The values of the coefficients are listed in Table 1.

For the DOBAMBC we have also listed the values as obtained by Huang and Dumrongrattana (*12*) and Carlsson *et al.* (*34*). The difference in sign in some of the parameters is due to the fact that in Carlsson *et al.* (*34*) the model predicts q (wavevector) to change sign at some temperatures, describing a transformation from a right handed (RH) to a left handed (LH) type of helix. The parameters as obtained by us and by Huang and Dumrongrattana (*12*) correspond to the RH (+) variant of DOBAMBC.

We have obtained three coefficients, Λ, d and f, by fitting to the experimental data of the temperature variation of the helical pitch [Equation (4)]. For DOBAMBC we obtain the values of a_2, a_4 and a_6 by fitting to the heat capacity data; the values of these constants are almost the same as those of Huang and Dumrongrattana (*12*). Taking these values of the parameters, Λ, d, f, a_2, a_4 and a_6, the remaining coefficients (χ, K_3, e, η and Z) have been obtained by fitting to the experimental data of P_0 and θ_0. In case of DOBA-1-MPC we fixed the values of Λ, d and f from the pitch data and determined the values of remaining eight coefficients to the best fit to the temperature dependence of θ_0 and P_0. Taking these values of parameters we have calculated the values of P_0, θ_0 and p as a function of temperature by solving simultaneously Equations (4)–(6). We find that the theoretical and experimental values of P_0 and θ_0 are in very good agreement for both the mesogens over the entire temperature region. However, near the

Table 1. Values of the Landau coefficients of the generalized mean-field model.

		Compounds			
		DOBAMBC			
Landau parameters	Units	This work	Ref. (*12*)	Ref. (*34*)	DOBA-1-MPC
a_2	$J\,m^{-3}\,K^{-1}$	4.52×10^4	4.52×10^4	3.50×10^4	4.05×10^5
a_4	$J\,m^{-3}$	5.25×10^5	5.25×10^5	8.00×10^5	6.02×10^6
a_6	$J\,m^{-3}$	8.83×10^6	8.83×10^6	9.00×10^6	4.10×10^6
χ	$10^{-11}\,F\,m^{-1}$	2.60	2.60	2.70	1.98
K_3	$10^{-12}\,N$	2.50	2.50	3.40	2.70
Λ	$10^{-5}\,J\,m^{-2}$	2.35	2.30	−1.40	1.20
d	$10^{-5}\,J\,m^{-2}$	2.48	2.50	−7.00	2.05
f	V	−0.23	−0.22	−0.21	−0.30
e	$10^{11}\,J\,m\,C^{-2}$	5.66	5.70	9.40	1.70
η	$10^{19}\,J\,m^5\,C^{-4}$	3.82	3.80	2.20	5.70
Z	$10^6\,V\,m^{-1}$	2.78	2.80	−41.00	3.05
T_c	K	367.5	367.6	–	359.0

peak of the helical pitch the theoretical result is about 5% above the measured data. As the value of $T_c - T$ increases the theoretical and experimental results differ slightly by about 3%. With these values of P_0, θ_0 and p and the measured data of $\Delta\in_G$ and f_G we obtained the values of K_3 and γ_G from Equations (36) and (37). The theoretical results are compared with the experimental data (see Figures 2–7).

In order to analyse the relative importance of each individual term of the generalised mean-field model, we evaluated the contribution of each term to the total free energy density at three values of $T_c - T = 1.0\,K$, $5.0\,K$ and $10.0\,K$; the results are given in Tables 2 and 3 for DOBAMBC and DOBA-1-MPC, respectively.

It is obvious from these tables that the first three terms involving coefficients a_2, a_4 and a_6 are the dominant ones in the expansion of the free-energy density. At each temperature the magnitudes of these terms decrease showing a convergence of the expansion series. The relative significance of the P_0^4 and $P_0^2\theta_0^2$ terms as compared to the terms P_0^2, $q\,\theta_0^2$, $q\,P_0\theta_0$ and $q^2\theta_0^2$ can obviously be seen. Further, in the vicinity of the SmA–SmC* transition both the bilinear coupling and the biquadratic coupling terms determine the properties of the system. As the

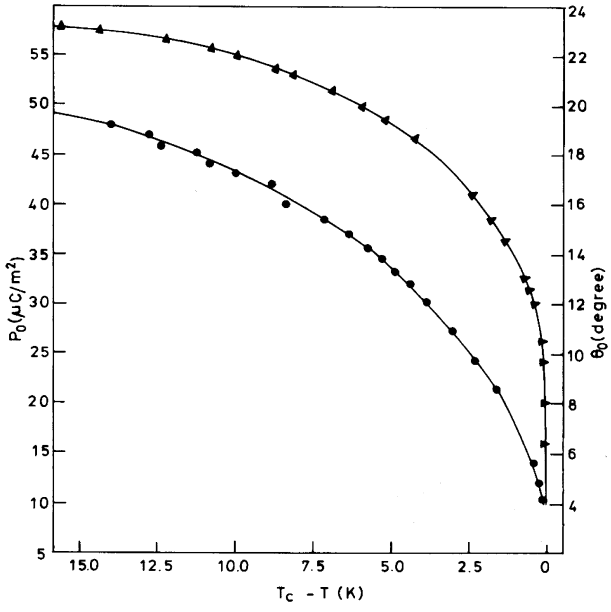

Figure 2. Comparison of the theoretical results (solid lines) with the experimental data (*21*) (denoted by filled circles for P_0 and filled triangles for θ_0) of the temperature variation of P_0 and θ_0 for DOBAMBC.

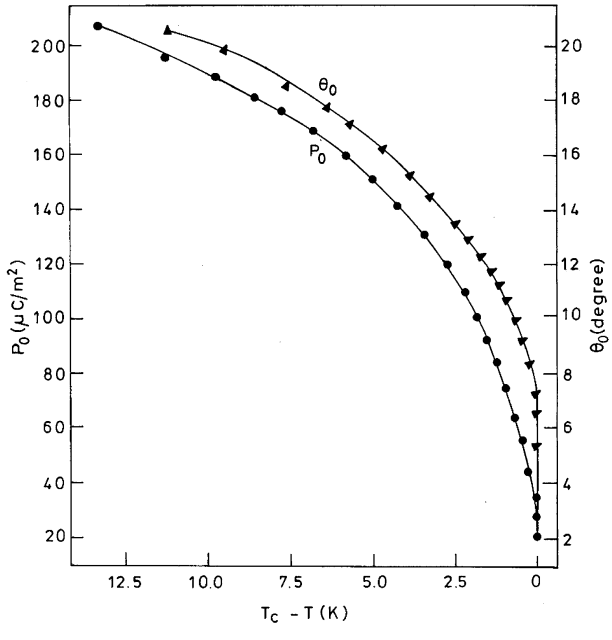

Figure 3. Comparison of the theoretical results with the experimental data (*21*) of the temperature variation of P_0 and θ_0 for DOBA-1-MPC. The symbols are same as those of Figure 2.

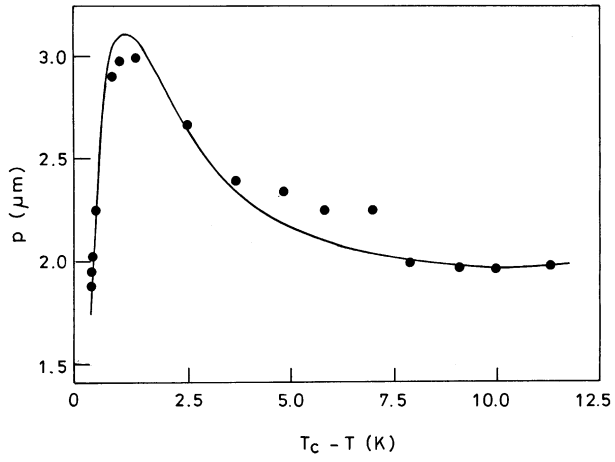

Figure 4. The temperature variation of helical pitch for DOBAMBC. Solid lines and filled circles represent, respectively, the theoretical results and the experimental data (*21*).

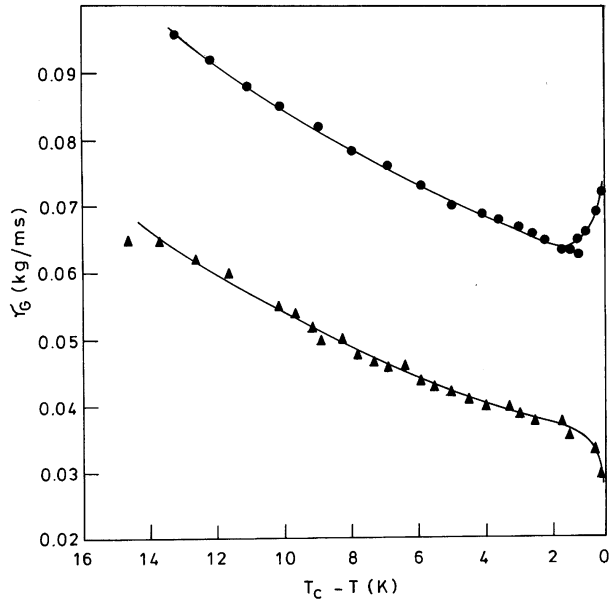

Figure 6. The temperature variation of Goldstone mode rotational viscosity γ_G for DOBAMBC [experimental data (*21*) filled triangles; theoretical result solid line] and DOBA-1-MPC [experimental data (*21*) filled circles and theoretical result solid line].

temperature decreases these coupling terms (involving Z and e coefficients) become more significant. The contribution of the Lifshitz invariant term (involving Λ) that is responsible for the helical pitch is small as compared to the terms involving tilt, polarisation and coupling between the tilt and polarisation but is still very significant as compared to the other remaining terms. As shown elsewhere (*37, 43*) in order to explain the SmA–SmC* transition properties a θ_0^6 term is required. A comparison between Tables 2 and 3 shows that at each temperature the effect of the terms involving P_0^2, P_0^4, $P_0\theta_0$ and $P_0^2\theta_0^2$ is more significant in case of DOBA-1-MPC as compared to DOBAMBC. However, $q\,\theta_0^2$, $q^2\theta_0^2$ and $q\,\theta_0^4$ terms contribute slightly more in case of DOBAMBC.

The temperature dependence of the polarisation, tilt angle and pitch are shown in Figures 2–5 for both mesogens. It can be seen that the theoretical results agree very well with the experimental data including the helical pitch. The anomalous behaviour of the pitch with temperature is found; at low temperature it slowly increases with increasing temperature, reaching a maximum at approximately 1 K below T_c, and then slowly decreases to a finite value at T_c. The behaviour of p as a function of θ_0 is such that p starts from a finite value at T_c, decreases towards a minimum approximately 1 K below T_c and then slowly increases with increasing the value of θ_0. In

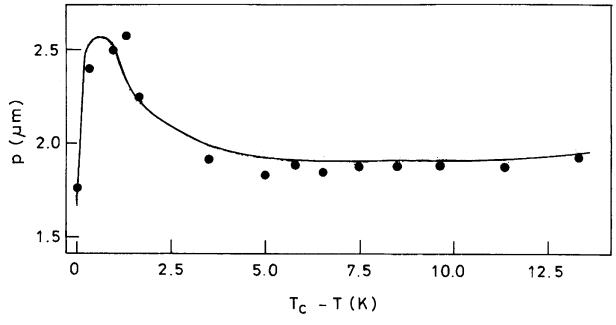

Figure 5. The temperature variation of helical pitch for DOBA-1-MPC (*21*). The symbols are same as those of Figure 4.

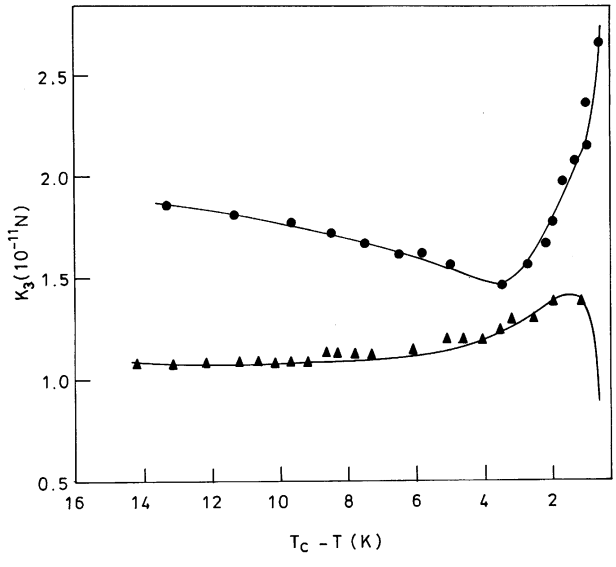

Figure 7. The temperature variation of the twist elastic constant K_3 for DOBAMBC and DOBA-1-MPC (*21*). The symbols are same as those of Figure 6.

Table 2. The magnitude of each individual term (in unit of $J\,m^{-3}$) of the generalised mean-field model [Equation (3)] and of P_0, θ_0 and q at three values of T_c-T for DOBAMBC.

	T_c-T		
	1.0 K	5.0 K	10.0 K
$\frac{1}{2}a_2(T_c-T)\theta_0^2$	0.13×10^4	1.11×10^4	3.33×10^4
$\frac{1}{4}a_4\theta_0^4$	0.044×10^4	0.128×10^4	0.285×10^4
$\frac{1}{6}a_6\theta_0^6$	0.002×10^4	0.141×10^4	0.069×10^4
$\frac{1}{2\chi}P_0^2$	5.6	23.55	34.7
$\frac{1}{4}\eta P_0^4$	0.798	14.33	31.2
$ZP_0\theta_0$	11.3	30.56	45.3
$\frac{1}{2}eP_0^2\theta_0^2$	4.7	34.18	75.0
$\Lambda q\,\theta_0^2$	2.833	6.772	10.88
$\frac{1}{2}K_3q^2\theta_0^2$	0.333	1.052	1.817
$d\,q\,\theta_0^4$	0.173	0.705	1.690
$f\,q\;P_0\;\theta_0$	1.971	7.383	11.786
$P_0/\mu C\,m^{-2}$	17.0	35.0	42.5
θ_0/rad	0.24	0.314	0.384
q/m^{-1}	2.10×10^6	2.92×10^6	3.14×10^6

fact, the anomaly in p is found to be closely related to the anomaly in the ratio P_0/θ_0.

In Figure 6 we compare the theoretical results for the temperature variation of the Goldstone mode rotational viscosity, γ_G, with the experimental (*21*) values for DOBAMBC and DOBA-1-MPC.

For both systems, the results for the twist elastic constant K_3 are plotted in Figure 7. In the numerical calculations of these quantities the theoretical values for the p, P_0 and θ_0 have been used. We found that the results of our calculations are in good agreement with the experimental data. In accordance with the experimental findings, we find in our calculations a bump near T_c in the curves of γ_G and K_3. It is believed (*21*) that the existence of bump is mainly related to the difficulties of determining the maximum of the Goldstone mode, dielectric strength $\Delta\in_G$ accurately.

Table 3. The magnitude of each individual term (in unit of $J\,m^{-3}$) of the generalised mean-field model [Equation (3)] and of P_0, θ_0 and q at three values of T_c-T for DOBA-1-MPC.

	T_c-T		
	1.0 K	5.0 K	10.0 K
$\frac{1}{2}a_2(T_c-T)\theta_0^2$	0.75×10^4	6.94×10^4	24.66×10^4
$\frac{1}{4}a_4\theta_0^4$	0.215×10^4	0.707×10^4	2.23×10^4
$\frac{1}{6}a_6\theta_0^6$	0.001×10^4	0.022×10^4	0.015×10^4
$\frac{1}{2\chi}P_0^2$	1.458×10^2	6.464×10^2	9.21×10^2
$\frac{1}{4}\eta P_0^4$	4.754×10^2	9.338×10^3	18.96×10^3
$ZP_0\theta_0$	0.445×10^2	1.278×10^2	2.033×10^2
$\frac{1}{2}eP_0^2\theta_0^2$	0.181×10^2	1.492×10^2	3.777×10^2
$\Lambda q\,\theta_0^2$	1.110	2.955	4.590
$\frac{1}{2}K_3\,q^2\theta_0^2$	8.437	1.193	1.621
$d\,q\,\theta_0^4$	0.069	0.346	0.955
$f\,q\;P_0\;\theta_0$	10.994	45.140	62.790
$P_0/\mu C\,m^{-2}$	76.0	160.0	191.0
θ_0/rad	0.192	0.262	0.349
q/m^{-1}	2.50×10^6	3.59×10^6	3.14×10^6

4. Summary and conclusion

A generalised (extended) mean-field model for the thermodynamic and phase transition properties of ferroelectric liquid crystals has been used to calculate the temperature variations of the tilt angle, spontaneous polarisation, helical pitch, Goldstone mode rotational viscosity and twist elastic constant in the SmC* phase near the SmA–SmC* transition in ferroic mesogens DOBAMBC and DOBA-1-MPC. The basis of the model is the Landau expansion of the free-energy density given by Equation (3). This expansion introduces 11 material parameters into the problem. In order to determine a complete set of these parameters we have adopted the usual procedure. For both the materials, we have determined the values of the coefficients Λ, d and f by the best fit to the experimental data of the helical pitch. In case of DOBAMBC we get the values of a_2, a_4 and a_6 by fitting to the heat capacity data. Taking these values of the parameters Λ, d, f, a_2, a_4 and a_6, the remaining coefficients (χ, K_3, e, η and Z) have been obtained by fitting to the experimental data of P_0 and θ_0. For DOBA-1-MPC, we determined the values of the coefficients a_2, a_4, a_6, χ, K_3, e, η and Z from the best fit to the temperature dependence of θ_0 and P_0. Using these coefficients, we have evaluated the values of the spontaneous polarisation, tilt angle, pitch, Goldstone mode rotational viscosity and the twist elastic constant as a function of temperature. We have also analysed the relative importance of each individual term of the free-energy density expansion [Equation (3)] by evaluating the respective contributions at three temperatures $T_c-T=1.0$ K, 5.0 K and 10 K for both mesogens. We have found that inclusion of terms involving θ_0^6, P_0^2, P_0^4, $P_0\theta_0$, $P_0^2\theta_0^2$ and $q\,\theta_0^2$ in the expansion is essential to explain the characteristic features of the SmC* phase near the SmA–SmC* transition.

We have compared the theoretical results with the experimental values and found a close agreement. In conclusion, using the generalised mean-field model we have been successful in explaining the characteristic features of the SmC* phase near the SmA–SmC* transition in the ferroic mesogens DOBAMBC and DOBA-1-MPC. However, we would like to emphasise that an answer at the microscopic level must be found to the question why the higher order terms are

so important in determining the properties of SmC* phase near the SmA–SmC* transition.

Acknowledgements

We are grateful to the University Grants Commission (UGC), New Delhi and the Department of Science and Technology (DST), New Delhi for financial support.

References

(1) Goodby J.W., Blinc R., Clark N.A., Lagerwall S.T., Osipov M.A., Pikin S.A., Sakurai T., Yoshino K., Zeks B. (Eds), *Ferroelectric Liquid Crystals: Principles, Properties and Applications.* Gordon and Breach Science: 1991, 1999.
(2) Lagerwall S.T. *Ferroelectric and Antiferroelectric Liquid Crystals*; Wiley-VCH: Weinheim, 1999.
(3) Harris A.B.; Kamien R.D.; Lubensky T.C. *Rev. Mod. Phys.* **1999**, *71*, 1745–1757.
(4) Bahr C., In *Chirality in Liquid Crystals*; Kitzerow H.S., Bahr C. (Eds), Springer-Verlag: New York, 2001, Chapter 8, pp. 225–250.
(5) Singh S. *Liquid Crystals: Fundamentals.* World Scientific: 2002, Chapter 9, pp. 370–452.
(6) Oswald P.; Pieranski P. *Smectic and Columnar Liquid Crystals*; Taylor and Francis: London, 2006, Chapter CIV, pp. 189–249.
(7) Clark N.A.; Lagerwall S.T. *Appl. Phys. Lett.* **1980**, *36*, 899–901.
(8) Lagerwall S.T.; Clark N.A.; Dijon J.; Clerc J.F. *Ferroelectrics* **1989**, *94*, 3–62.
(9) Meyer R.B.; Liebert L.; Strzelecki L.; Keller P. *J. Phys. Lett., Paris* **1975**, *36*, L69–L71.
(10) Martinot-Lagarde P.H.; Duke R.; Durand G. *Mol. Cryst. liq. Cryst.* **1981**, *75*, 249–286.
(11) Musevic I.; Zeks B.; Blinc R.; Wyder P. *Ferroelectrics* **1984**, *58*, 71–77.
(12) (a) Dumrongrattana S.; Huang C.C. *Phys. Rev. Lett.* **1986**, *56*, 464–467; (b) Dumrongrattana, S.; Huang, C.C.; Nounesis, G.; Lien, S.C.; Viner, J.M. *Phys. Rev. A* **1986**, *34*, 5010–5019.
(13) Musevic I.; Blinc R.; Zeks B.; Filipic C.; Copic M.; Seppen A.; Wyder P.; Levanyuk A. *Phys. Rev. Lett.* **1988**, *60*, 1530–1533.
(14) Qiu R.; Ho J.T.; Hark S.K. *Phys. Rev. A* **1988**, *38*, 1653–1655.
(15) Skarabot M.; Blinc R.; Musevik I.; Rostegar A.; Rasing T. *Phys. Rev. E* **2000**, *61*, 3961–3968.
(16) Uehara H.; Hatano J. *Mol. Cryst. Liq. Cryst.* **2001**, *366*, 525–532.
(17) Yoshimitsu H.; Tamura Y.; Hachida M. *Ferroelectrics* **2007**, *348*, 144–148.
(18) Levstik A.; Kutnjak Z.; Zeks B.; Dumrongrattana S.; Huang C.C. *J. Phys., Paris II* **1991**, *1*, 797–803.
(19) Ghoddoussi F.; Pantea M.A.; Keyes P.H.; Naik R.; Vaishnava P.P. *Phys. Rev. E* **2003**, *68*, 051706–14.
(20) Kutnjak Z. *Phys. Rev. E* **2004**, *70*, 061704–15.
(21) Levstik A.; Kutnjak Z.; Filipic C.; Levstik I.; Breger Z.; Zeks B.; Carlsson T. *Phys. Rev. A* **1990**, *42*, 2204–2210.
(22) Giesselmann F.; Zugenmaier P. *Phys. Rev. E* **1995**, *52*, 1767–1772.
(23) Raina K.K.; Ahuja J.K. *Mol. Cryst. Liq. Cryst.* **1998**, *325*, 157–171.
(24) Yang K.H.; Chieu T.C.; Osofsky S. *Appl. Phys. Lett.* **1989**, *55*, 125–127.
(25) Bahr C.; Heppke G. *Phys. Rev. A* **1990**, *41*, 4335–4342.
(26) Olbrich E.; Marinov O.; Davidov D. *Phys. Rev. E* **1993**, *48*, 2713–2720.
(27) O'Brien J.P.; Moses T.; Chien W.; Freysz E.; Ouchi Y.; Shen Y.R. *Phys. Rev. E* **1993**, *47*, R2269–R2272.
(28) Link D.R.; Maclennan J.E.; Clark N.A. *Phys. Rev. Lett.* **1996**, *77*, 2237–2240.
(29) Pandey M.B.; Dhar R.; Agrawal V.K.; Khare R.P.; Dabrowski R. *Phase Transitions* **2003**, *76*, 945–958.
(30) Thakur A.K.; Chadha G.K.; Kaur S.; Bawa S.S.; Biradar A.M. *J. Appl. Phys.* **2005**, *97*, 113514–20.
(31) Pikin S.A.; Indenbom V.L. *Soviet Phys. Usp.* **1978**, *21*, 487–501.
(32) Huang C.C.; Dumrongrattana S. *Phys. Rev. A* **1986**, *34*, 5020–5026.
(33) Zeks B. *Mol. Cryst. Liq. Cryst.* **1984**, *114*, 259–270.
(34) Carlsson T.; Zeks B.; Filipic C.; Levstik A.; Blinc R. *Mol. Cryst. Liq. Cryst.* **1988**, *163*, 11–72; and references therein.
(35) Levstik A.; Carlsson T.; Filipic C.; Levstik I.; Zeks B. *Phys. Rev. A* **1987**, *35*, 3527–3534.
(36) Carlsson T.; Zeks B. *Liq. Cryst.* **1989**, *5*, 359–365.
(37) Huang C.C.; Viner J.M. *Phys. Rev. A* **1982**, *25*, 3385–3388.
(38) Carlsson T.; Dahl I. *Mol. Cryst. Liq. Cryst.* **1983**, *95*, 373–400.
(39) Levstik A.; Kutnjak Z.; Levstik I.; Zeks B., In *Proceedings of the Seventh International Meeting on Ferroelectricity*, Saarbrucken, 1989.
(40) Xue J.Z.; Handschy M.A.; Clark N.A. *Ferroelectrics* **1987**, *73*, 305–314.
(41) Sharp K.; Flatischler K.; Lagerwall S.T. *Ferroelectrics* **1988**, *84*, 183–195.
(42) Escher C.; Geelhaur T.; Bohm E. *Liq. Cryst.* **1988**, *3*, 469–484.
(43) Bescari P.; Calderer M.C.; Terentjev E.M. *Phys. Rev. E* **2007**, *75*, 051707–18.